EUROPEAN CONFERENCE ON INTEGRATED OPTICS

Optical isolator element using nano-pixel for photonic integrated circuits

Haisong Jiang, Cangui Tang, and Kiichi Hamamoto

Interdisciplinary Graduate School of Engineering Sciences, Kyushu University,
6-1, Kasuga-koen, Kasuga, Fukuoka 816-8580, Japan
* jiang.haisong.447@m.kyushu-u.ac.jp

On-chip optical isolators are highly required components and have been researched and developed in optical communication system. In this study, we have proposed an integration-available ultra-compact isolator element based on nano-pixel configuration. The footprint of isolator element is designed in 3.0 × 3.0 μm^2. The simulated result exhibited superior an isolation ratio of 16.3 dB with excess loss of 1.2 dB at 1550 nm wavelength.
Keywords: *Nano-pixle, Isolator*

INTRODUCTION

In recent years, low-loss and high-performance photonic integrated circuits (PICs) have been researched widely for optical communication systems [1]. Among on-chip optical components, integrated optical nonreciprocal devices, such as optical isolators and circulators, which block the back-reflected light to protect optical systems, are still missing elements in current PICs. Previously, integrated optical isolators based on magneto-optical effects [2-3], nonlinear photonic effects [4-5] and spatiotemporal modulation [6-7] have been reported, however, they are not well deployed in several reasons including performance, processing difficulty, and others. In this paper, we newly propose an integrated isolator element based on optical nano-pixel waveguide configuration. The nano-pixel structure waveguide attracts attention recently as new optical waveguide device structure [8-10] because of the compact design capability. In addition, nano-pixel structures manage to influence the spatial properties of the optical field, including its amplitude, polarization, and phase distribution and we have proposed and demonstrated asymmetric power coupler [11], higher-order modes compressor [12], spot size convertor [13] based on nano-pixel waveguide configuration. In this work, we newly propose an integration-available isolator element based on nano-pixel waveguide configuration for PICs. The footprint is ultra compact of 3.0 × 3.0 μm^2. By optimizing the number and the position of the nano-pixel arrangement using direct binary search (DBS) [14], an isolation ratio of 16.3 dB with excess loss of 1.2 dB at 1550 nm wavelength has been successfully confirmed using FDTD (finite-difference time-domain) simulation.

CONCEPT

Nano-pixel is consisted of a rectangular waveguide region which is divided into small pixels with around a hundred nano-meter scale. Each pixel is set with single digit binary data. The actual pixel is selected to be “1” or “0”, which means fully occupied with the waveguide material (corresponding to 1) or void (corresponding to 0). And in this work, “air-hole” is introduced for the void case. One of the merits of this nano-pixel structure is the device size. Many of the reported devices [14-25] are in the dimension of several micrometer squares in the footprint. Figure 1 (a) shows the schematic of the proposing isolator element using nano-pixel configuration. Once light is injected into the nano-pixel waveguide region, the designed pixel arrangement with the combination of occupied and void causes

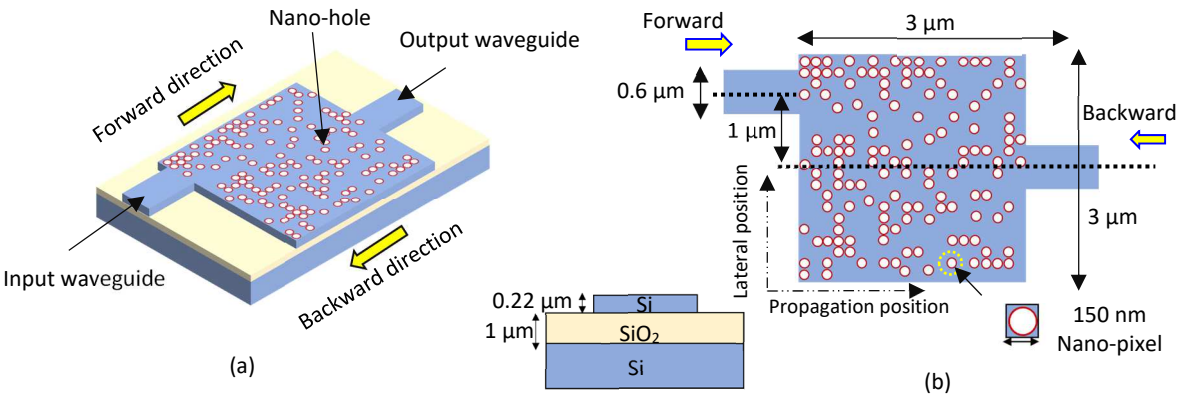

Fig. 1 The structure of isolator element using nano-pixel. (a) The schematic of isolator element, and (b) the configuration of isolator element.

the light scattering, and the scattered light in the optical waveguide interferes with each other. By setting the lateral position of the input waveguide and the output waveguide differently and choosing the number and the position of the air hole arrangement, the light interference in the forward direction and the return direction will be different. Especially the input and output waveguide layout against nano-pixel waveguide region is one of the keys of the isolation characteristics. We are based on the reciprocal propagation property caused in nano-pixel waveguide region. This phenomenon is not common in ordinal optical waveguide. To cause this reciprocal effect, the input for the forward light is located at laterally far side from the center whereas the output is located at the center of the nano-pixel waveguide region (see Fig. 1).

DESIGN AND OPTIMIZATION

The waveguide geometries are indicated in Fig. 1 (b). A single-mode waveguide with a width of 0.6 µm and a length of 1 µm is connected to the left and the right of the nano-pixel waveguide region. The output port is connected to the lateral center of nano-pixel waveguide region, and the input port is connected to 1 µm away from lateral center of nano-pixel waveguide region. The nano-pixel waveguide region has the waveguide width and length of 3 µm each which corresponds to the footprint of 3 × 3 μm^2. The nano-pixel waveguide region is divided into square nano-pixel sections. Each section is designed as square with 150 nm in the side-length. Circular air holes are arranged in void with 130 nm diameter. Totally 400 nano-pixel sections are arranged (which corresponds to 20 × 20 sections) in the nano-pixel waveguide region. Since each hole is cylindrical and filled with air for the void case in the nano-pixel, the refractive index is set to be 1 at the hole-area in simulation. The layer structure was a strip waveguide with Si core layer on top of SiO2 cladding layer. The thickness of the Si core layer was set to be 0.22 µm, and the thickness of the under cladding-layer was set to be 1 µm.

As explained above, the nano-pixel waveguide region is divided into 400 sections, these are too many possible layouts. Since it is not realistic to simulate all of the possible layouts and verify the results, we have designed the nano-pixel waveguide by using dual binary scarch (DBS) [14] algorithm in this work. 2D FDTD method with injected light of 1550 nm (TE-mode) was used in the simulation. The nano-pixel structure pattern is considered as a matrix contributed by 0 and 1, in which 1 corresponds to waveguide material whereas 0 corresponds to void. A randomly chosen pixel is first perturbed so as to switch its state, then device characteristic is calculated. If the characteristic is improved, the pixel state is retained, if not, the perturbation is reversed and the algorithm proceeds to the next pixel. This process is continued until the target characteristic is obtained. The characteristic of the device is defined as the isolation ratio. The isolation ratio τ is defined as:

$$\tau = 10*\log10\,[(Pout1 / Pout2] \qquad (1),$$

where Pout1 and Pout2 are the output power in the forward direction and backward direction, respectively. In this optimization process, CPU of the PC was Intel (R) Core (TM) i9-10940X CPU @ 3.30 GHz and RAM was 128 GB. It took approximately 120 hours to design and optimize the device in this work.

RESULT

After optimization process, we have got the isolator element using nano-pixel configuration. 138 holes are arranged inside optimized isolator element with 3.0 µm × 3.0 µm nano-pixel waveguide. Figure 2 shows the electromagnetic field of light of optimized isolator element in forward direction and backward direction. It is clearly shown that the output in forward direction high whereas output in backward direction is quite low. Figure 3 shows the normalized output power of optimized isolator element in forward direction and backward direction during the FDTD simulations shown in Fig. 2. The horizontal axis shows time and [fs] represents 10-15s. The vertical axis shows the

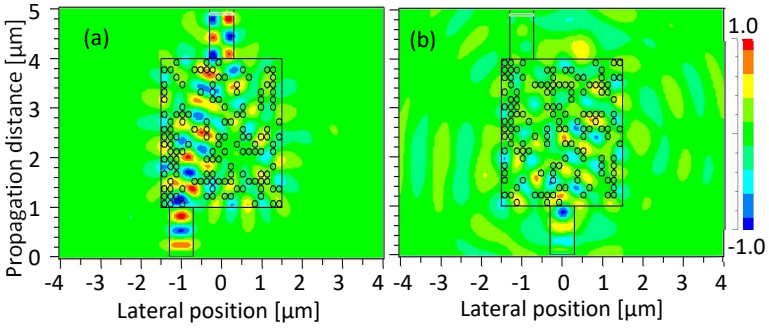

Fig. 2 The electromagnetic field of light of optimized isolator element. (a) In forward direction and (b) in backward direction.

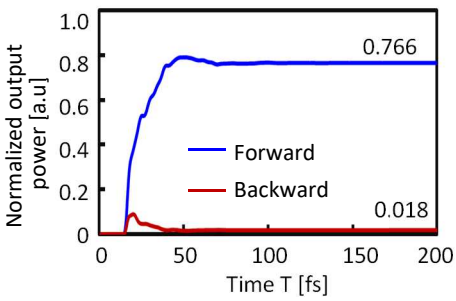

Fig. 3 The normalized output power of optimized isolator element.

output of light, and since it is normalized by the incident light, it takes a value of 0 to 1. The output power of the isolator in the forward direction is 0.766 whereas the one in backward is 0.018, respectively. An isolation ratio of 16.3 dB and with 1.2 dB of excess loss using nano-pixel structure was achieved.

We also investigated the wavelength dependence of isolation ratio for the isolator element. Figure 4 shows the calculated transmission spectra of isolator with TE-mode. As shown in the Fig. 4, more than 15 dB of isolation ratio was confirmed from 1540 nm to 1560 nm of wavelength. The 1 dB bandwidth of this device was 20 nm, and across the entire 1 dB bandwidth, the device excess loss was 1.2~ 1.3 dB.

Fabrication accuracy for nano-hole is another important challenge for isolator element based on nano-pixel configuration. Herein, we also analyzed the isolation ratio of the proposed isolator element based on nano-pixel configuration with the change of the air hole diameter. When we change the diameter of the hole from 120 to 150 nm, therefore, the space of the holes is simultaneously adjusted from 40 to 0 nm. Figure 5 shows the calculated isolation ratio with different diameters. As shown in Fig. 5, there is less effect on the isolation ratio due to the nano-pixel hole fabrication errors. More than 15 dB of isolation ratio was confirmed from 125 nm to 140 nm of nano-hole diameters.

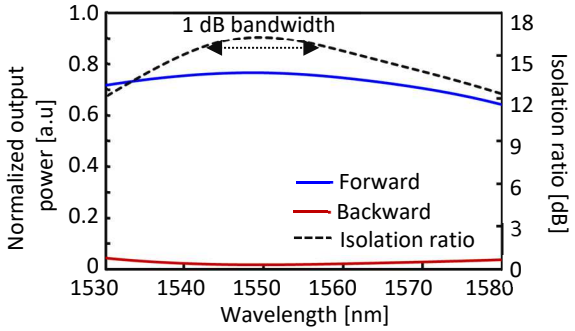

Fig. 4 The calculated transmission spectra of isolator element.

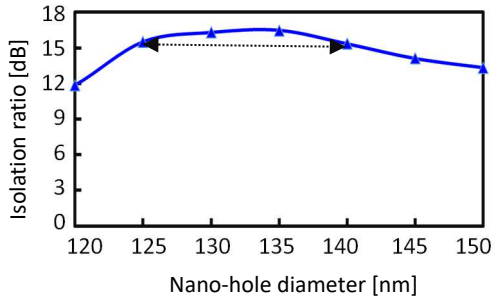

Fig. 5 The calculated isolation ratio with different diameters.

CONCULUTION

We have proposed an integrated isolator element based on nano-pixel waveguide. The isolator element with a small footprint of 3.0 × 3.0 μm^2 has been designed and optimized by DBS algorithm. By optimizing the number and the position of the nano-pixel arrangement, an isolation ratio of 16.3 dB with excess loss of 1.2 dB at 1550 nm wavelength has been confirmed. This paper is intended to report the possibility of isolator using nano-pixel for the first time as to our knowledge, and still there is a number of possibility in achieving higher performance when we change the size, the number of air-holes, as well as the waveguide configuration.

References

[1] D. Marpaung et al., Integrated microwave photonics. Laser Photonics Rev., vol. 7, no. 4, pp. 506-538, 2013
[2] R. Yamaguchi et al., Low-loss waveguide optical isolator with tapered mode converter and magneto-optical phase shifter for TE mode input, Opt. Express vol. 26, no. 16, pp. 21271-21278, 2018
[3] S. Liu et al., TE-mode magneto-optical isolator based on an asymmetric microring resonator under a unidirectional magnetic field, Opt. Express vol. 30, no. 6, pp. 9934-9943, 2022
[4] L. Fan et al., An all-silicon passive optical diode, Science, vol. 335, no. 6067, pp. 447-450,2012
[5] Y. Shi et al, Limitations of nonlinear optical isolators due to dynamic reciprocity, Nat. Photonics vol. 9, pp. 388-392, 2015
[6] J. Wang et al., Non-reciprocal polarization rotation using dynamic refractive index modulation, Opt. Express, vol. 28, no. 8, pp. 11974-11982, 2020
[7] E. A. Kittlaus, et al, Nonreciprocal inter-band brillouin modulation, Nat. Photonics vol.12, pp. 613-619, 2018
[8] B. Shen et al., An integrated-nano photonics polarization beam splitter with 2.4×2.4 μm^2 footprint, Nat. Photonics, vol. 9, pp. 378-382, 2015
[9] J. Huang et al., Digital nanophotonics: the highway to the integration of subwavelength-scale photonics, Nanophotonics vol. 10, no. 3, pp. 1011-1030, 2021
[10] Y., Shimamura et al., First implementation of asymmetric power splitter by using nano-pixel integrated with sensing high-mesa waveguide, in Tech. Digest of 27th Microoptics Conference, Jena, Germany, pp. 41-42, 2022
[11] H. Jiang et al., Demonstration of space-mode “compressor” by using nano-pixel, in Tech. Digest of 27th Microoptics Conference, Jena, Germany, pp. 60-61, 2022
[12] Chen et al., Vertical field enhancement of a spot-size converter using a nanopixel waveguide and window structure. Opt. Express, vol. 29, no. 2, pp. 2757-2768, 2021
[13] W. Chang et al., Ultra-compact mode (de) multiplexer based on subwavelength asymmetric Y-junction, Opt. Express, vol. 26, no. 7, pp. 8162-8170, 2018
[14] K. Nakamura et al., Hybrid algorithm based on the grey wolf optimizer and direct binary search for the efficient design of a mosaic-based device, J. Opt. Soc. Am. , vol. B39, no. 5, pp. 1329-1337, 2022